Dispersion of Cascaded Fiber Gratings in WDM Lightwave Systems

Natalia M. Litchinitser, Benjamin J. Eggleton, and Govind P. Agrawal, *Fellow, IEEE, Fellow, OSA*

***Abstract*— Fiber gratings operating in the transmission mode can provide high dispersion at wavelengths close to the Bragg resonance. When multiple gratings are cascaded for wavelength division multiplexing (WDM) applications, the net dispersion between the stop bands of any two consecutive gratings is significantly modified. We discuss the dispersion characteristics of such cascaded fiber gratings and propose a dispersion compensator for simultaneous compensation of group-velocity dispersion (GVD) for multiple channels of a WDM lightwave system. We also discuss the impact of the dispersion possessed by cascaded gratings on grating based add–drop multiplexers.**

***Index Terms*— Dispersion compensation, fiber gratings, wavelength division multiplexing.**

I. Introduction

FIBER gratings are emerging as one of the most important components for designing fiber-optic communication systems. They are likely to have application in two main areas: dispersion compensation in long-haul fiber networks [1]–[3] and wavelength routing in wavelength division multiplexed (WDM) lightwave systems [4], [5]. In both of these areas, grating dispersion will impact the system performance.

Bragg gratings exhibit dispersion both in reflection, especially when the grating is chirped [2], and in transmission at wavelengths close to the stop band [3], [6]. At wavelengths close to the grating stop band, the group-velocity dispersion (GVD) of a fiber grating is many orders of magnitude larger than that occurring in standard optical fibers used for signal transmission. Recently, dispersion compensation by a transmission grating has been demonstrated in a 72-km fiber link leading to error-free transmission of a 10 Gbit signal [7]. We subsequently analyzed the performance of such transmission-based dispersion compensator employing a single apodized, unchirped fiber Bragg grating and found that nearly ideal pulse recompression can be achieved [3]. In a WDM network many channels need to be compensated simultaneously, and therefore the impact of total dispersion possessed by numerous gratings need to be examined.

The impact of dispersion is also important for dense WDM lightwave systems making use of grating-based add–drop filters. In such filters, fiber gratings add or drop a selected channel by reflecting it, while the neighboring channels are transmitted through the grating. Such transmitted channels are affected by the strong out-of-band dispersion possessed by the grating [8], [9]. Given that each channel may pass through numerous fiber gratings during its transmission, the degradation of the signal because of the out-of-band dispersion of fiber gratings may limit the bit rate or the transmission distance achievable.

In this paper, we generalize the results of [3] and [8] and consider the transmission of optical pulses through a WDM network incorporating cascaded fiber gratings. There are two motivations for our work. First, we show that by a careful arrangement of cascaded fiber gratings, simultaneous dispersion compensation for multiple WDM channels can be realized. Second, we consider the dispersive impact of grating-based add–drop filters, which typically make use of cascaded fiber gratings [5].

II. Dispersion of Cascaded Fiber Gratings

Before considering cascaded gratings, we first review the dispersion properties of an infinite, uniform, fiber Bragg grating. We note that the dispersion characteristics of an infinitely long grating are similar to those of a finite-length apodized grating [3]. To a good approximation, the grating dispersion can be described by the following dispersion relation of a periodic structure [3], which is obtained using the coupled-mode equations yielding [10], [11]:

$$\gamma^2 = \delta^2 - \kappa^2 \tag{1}$$

where $\delta = n(\omega - \omega_B)/c$ is the detuning of the channel carrier frequency ω from the resonant Bragg frequency ω_B, and $\gamma = \beta - \beta_B$ is the deviation of the propagation constant β from the Bragg wavenumber β_B, n is the mode index in a single-mode silica fiber, and c is the speed of light in vacuum. The coupling coefficient κ is defined in the usual manner. The grating stop band corresponds to detuned frequencies $|\delta| < \kappa$, where the reflectivity is high. At frequencies close to the stop band ($|\delta| > \kappa$), the grating exhibit strong second- and higher-order dispersion, which strongly affects the light propagation. On the short-wavelength side of the stop band ($\delta > 0$), where the dispersion is anomalous, Bragg solitons have been predicted and experimentally demonstrated [12], [13]. On the long-wavelength side ($\delta < 0$), the dispersion is normal and can be used for compensation of anomalous GVD of fibers in the 1.55-μm wavelength region [3], [7]. Clearly, at frequencies far from the stop band ($|\delta| \gg \kappa$) the grating plays no significant role, and the dispersion relation becomes identical to that of a uniform medium, i.e., $\gamma \approx \pm\delta$.

Manuscript received November 11, 1997; revised April 22, 1998.

N. M. Litchinitser and G. P. Agrawal are with The Institute of Optics, University of Rochester, Rochester, NY 14627 USA.

B. J. Eggleton is with Bell Laboratories, Lucent Technologies, Murray Hill, NJ 07974 USA.

Publisher Item Identifier S 0733-8724(98)05657-6.

We now consider a cascade of two gratings with Bragg frequencies ν_1 and ν_2 such that the frequency separation, $|\nu_1 - \nu_2| \equiv \Delta\nu$, is larger than the width of the stop band of each grating. Then, there is no spectral overlap and thus we can ignore interference effects between the gratings. We assume for simplicity that the coupling strength κ is the same for both gratings. The dispersion relation for the second grating can be written as

$$(\gamma + \Delta)^2 = (\delta + \Delta)^2 - \kappa^2 \tag{2}$$

where $\Delta = 2\pi n \Delta\nu / c$.

Following the approach of [3], [6] we find the following analytical expressions for the GVD coefficient β_2^g and third-order dispersion parameter β_3^g valid in the region between the stop bands of two uniform fiber gratings:

$$\beta_2^g = \left(\frac{n}{c}\right)^2 \left[\frac{\kappa^2}{[(\delta+\Delta)^2 - \kappa^2]^{3/2}} - \frac{\kappa^2}{(\delta^2 - \kappa^2)^{3/2}}\right] \times \mathrm{sign}(\delta) \tag{3}$$

$$\beta_3^g = 3\left(\frac{n}{c}\right)^3 \left[\frac{\kappa^2 \delta}{(\delta^2 - \kappa^2)^{5/2}} + \frac{\kappa^2(\delta+\Delta)}{[(\delta+\Delta)^2 - \kappa^2]^{5/2}}\right]. \tag{4}$$

Both expressions (3) and (4) diverge at the band edge of each grating, i.e., at $\delta = -\kappa$ and $\delta = \kappa - \Delta$. The GVD and third-order dispersion parameters, β_2^g and β_3^g for the two cascaded gratings, as well as those of individual gratings are shown in Figs. 1(a) and (b), respectively, as functions of the detuning parameter δ for a channel spacing of 100 GHz ($\Delta = 31.4$ cm^{-1}) after choosing $\kappa = 4$ cm^{-1} and $n = 1.5$. The solid curve in Fig. 1(a) shows that in the presence of another grating the GVD becomes zero at $|\delta| = \Delta/2$. Therefore, in contrast with the single grating case, there exists a zero-GVD wavelength. This zero-GVD wavelength can be easily shifted by varying the grating-design parameters κ and Δ. It is noteworthy that the third-order dispersion is always positive for each grating and, since the two contributions are additive between the stop bands, the total dispersion does not vanish at any wavelength as shown in Fig. 1(b). This feature is similar to that of standard telecommunication fibers for which the third-order dispersion is always positive as well [14]. As third-order dispersive effects can distort short optical pulses and have the potential of becoming detrimental for devices such as dispersion compensators and optical add–drop multiplexers, the ratio between the second- and third-order dispersion terms is often used as a figure of merit (FOM) for characterizing the performance of a fiber grating. We define the FOM as

$$F(\delta) = \left|\frac{\beta_2^g}{\beta_3^g} \sigma_0 \sqrt{2}\right| \tag{5}$$

where σ_0 is the transform-limited rms pulse width (for a Gaussian pulse, rms pulse width σ_0 is related to the $1/e$-width $T_{1/e}$ through $\sigma_0 = T_{1/e}/\sqrt{2}$). The rms width is used here since a Gaussian pulse does not maintain its shape after propagation in a medium with nonzero third-order dispersion. Fig. 2 shows how F varies with δ in the region between the stop bands of the two gratings for a channel spacing of 200 GHz ($\Delta = 62.8$ cm^{-1}). Note, that $F(\delta)$ vanishes at zero-GVD wavelength as well as near to either grating stop band as shown in Fig. 2. Clearly, to minimize the detrimental effects of third-order dispersion, F should be as large as possible for a given set of design parameters.

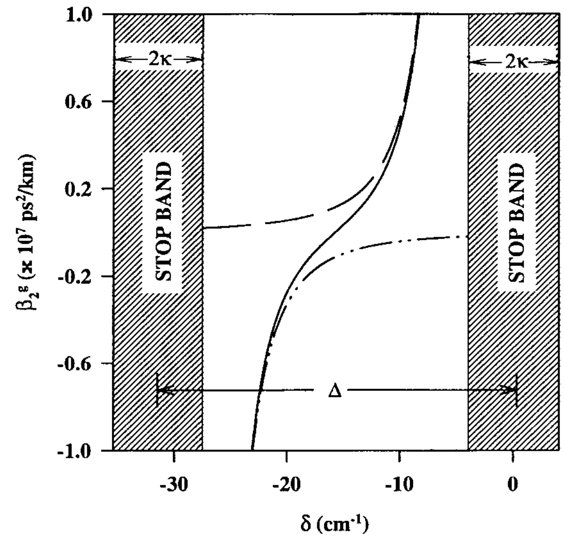

(a)

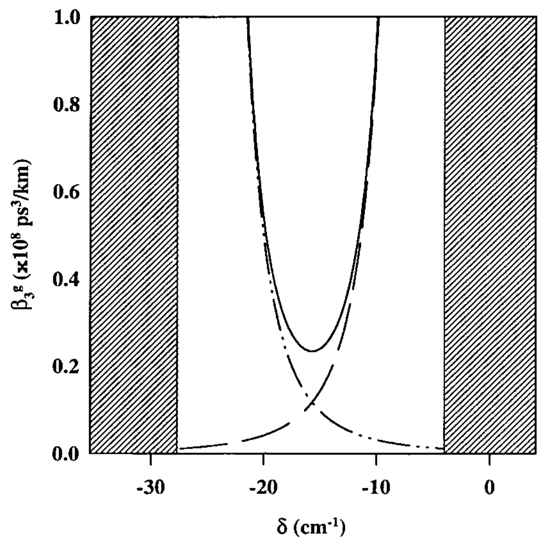

(b)

Fig. 1. (a) Group-velocity dispersion and (b) third-order dispersion as functions of δ for a single grating centered at $\delta = 0$ (dashed line) and $\delta = -\Delta$ (dot-dashed line), and for two cascaded gratings (solid line). The parameters used are $\kappa = 4$ cm^{-1}, $\Delta\nu = 100$ GHz (31.4 cm^{-1}).

III. WDM Applications of Cascaded Gratings

A. Dispersion Compensation in WDM Systems

We first apply the results of Section II to design a dispersion compensator for an N-channel WDM system after the WDM signal has been transmitted through standard telecommunication fiber. Dispersion compensation is achieved by N apodized, unchirped, fiber Bragg gratings operating in transmission as shown in Fig. 3. We assume that the channels in the WDM system are equally spaced by Δ. The analysis can be easily extended for an unequal channel spacing.

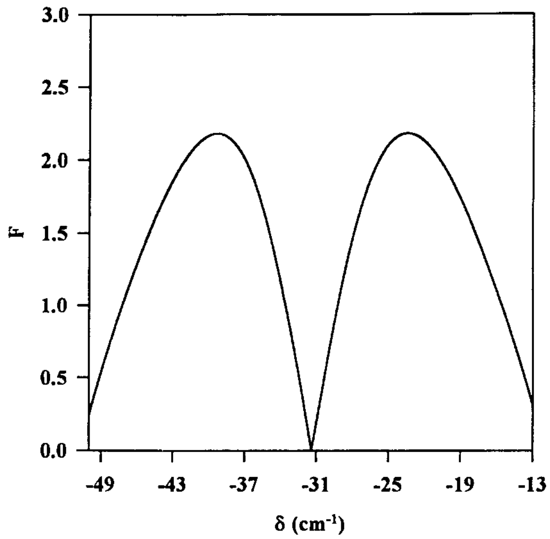

Fig. 2. Figure of merit F versus detuning for $\kappa = 12$ cm^{-1}, $\sigma_0 = 17$ ps, and $L_g = 40$ cm, for a 200-GHz channel spacing ($\Delta = 62.8$ cm^{-1}).

We assume that the channel spacing Δ is large compared to the pulse bandwidth and that the grating stop bands satisfy $2\kappa < \Delta$. Then, to a good approximation, we can consider only the effect of two consecutive gratings on transmission of any particular channel and neglect the effect of all other gratings. This approximation is valid in practice because the dispersion of each grating reduces significantly far away from its own stop band. To compensate for anomalous GVD of optical fibers at communication wavelengths, the normal-dispersion side of grating spectrum should be used, i.e., $|\omega_0| < |\omega_B|$ where $|\omega_0|$ is the central frequency of the channel under consideration. The nearest adjacent grating centered at $|\omega_B - (c/n)\Delta| < |\omega_0|$, exhibiting anomalous dispersion at ω_0 must also be considered as it will degrade the overall performance of the compensator.

In our model we consider propagation of an initially transform-limited Gaussian pulse of rms width σ_0 in an optical fiber of length L_f with dispersion β_2^f. A Gaussian pulse maintains its shape with propagation through the fiber, but its width increases because of GVD resulting in the rms width [14] $\sigma_1 = \sigma_0\sqrt{1 + (L_f/L_D)^2}$ where $L_D = 2\sigma_0^2/|\beta_2^f|$ is the dispersion length. The pulse also becomes linearly chirped with the chirp parameter $\alpha = L_f/\beta_2^f[1/(L_f^2 + L_D^2)]$.

Clearly, for an ideal dispersion compensator that recompresses the dispersion-broadened pulse to its original width, one must satisfy

$$\beta_2^g L_g = -\beta_2^f L_f \tag{6}$$

where L_g is the grating length and β_2^g is given by (3). We use a graphical approach to find the optimum detuning parameter δ_{opt} from (6). In Fig. 4 the left-hand side (solid line) and right-hand side (dashed line) of (6) are plotted for $\kappa = 4$ cm^{-1}, $L_g = 40$ cm, $\beta_2^f = -20$ ps^2/km, $L_f = 100$ km. The intersection of two lines provides a solution for δ_{opt}. Note that the stop band of one grating is centered at $\delta = 0$ and while that of the other is centered at $\delta = -\Delta = -31.4$ cm^{-1}.

By using (5) and (6) one can find the parameters of two adjacent gratings for optimum performance of the dispersion compensator. We describe the performance of the device in terms of input/output pulse-width ratio. Following the approach described in [15] the rms pulse width after propagating in a grating of length L_g can be found analytically for the case including quadratic and cubic dispersion. The ratio of initial pulse width σ_0 and recompressed pulse width σ_2, can be written as

$$\frac{\sigma_0}{\sigma_2} = \frac{\sigma_0}{\sigma_1}\left[\left(1 + \beta_2^g L_g \alpha\right)^2 + \left(\frac{L_g \beta_2^g}{2\sigma_1^2}\right)^2 + \left[1 + \left(2\alpha\sigma_1^2\right)^2\right]\frac{1}{8}\left(\frac{L_g \beta_3^g}{2\sigma_1^3}\right)^2\right]^{-1/2}. \tag{7}$$

This ratio is plotted in Fig. 5 for $\kappa = 4$ cm^{-1}, $\Delta = 31.4$ cm^{-1} (channel spacing 100 GHz) and $L_g = 40$ cm (solid line). The dashed line corresponds to the case when only one grating at $\delta = 0$ is used. Fig. 5 shows that because of the second grating at $\delta = -\Delta$, the maximum value of σ_0/σ_2 decreases slightly and the optimum value of δ increases slightly. However, at $\delta = \delta_{\text{opt}}$, where the peak occurs, the compensator performance is virtually unaffected by the second grating.

We have shown previously that the ratio σ_0/σ_2 in the single-grating case can always be improved by making gratings stronger and longer [3]. However, this is not always true when gratings are cascaded because of the fixed value of the channel spacing. To estimate the range of κ for which the detrimental effect of the adjacent grating is not excessive, we plot in Fig. 6 the figure of merit F as a function of the coupling strength κ for three values of channel spacing $\Delta\nu = 200$ GHz (solid line), 100 GHz (long dashed line), 50 GHz (dot-dashed line). As the channel spacing becomes smaller the recompressed pulse is affected more and more by the third-order dispersion effects. Also, the range of detunings for which the third-order dispersion is not excessive becomes narrower as $\Delta\nu$ decreases. The cascaded-grating compensator proposed here should work quite well for channel spacings as small as 100 GHz (about 0.8 nm at $\lambda = 1.55$ μm).

B. Dispersion in Cascaded-Grating Based Add–Drop Filters

We now use the analytical results obtained in Section II to analyze the performance of a fiber-grating-based add–drop filters. Recently, it was theoretically predicted and experimentally demonstrated that in dense WDM systems, with many closely spaced channels, out-of-band dispersion of a single fiber-grating filter may be detrimental for the adjacent channels that are transmitted through the grating [8], [9]. Here, we extend the analysis of [8] and consider the transmission of a given channel through cascaded gratings. As in previous subsection, we examine the impact of two nearest gratings on the transmitted channel. The main difference here is that the transmitted channel is located between the two stop bands (corresponding to two added/dropped channels) as shown in Fig. 7.

We assume that the input pulse is a transform-limited Gaussian pulse of rms-width σ_0. Pulse broadening induced

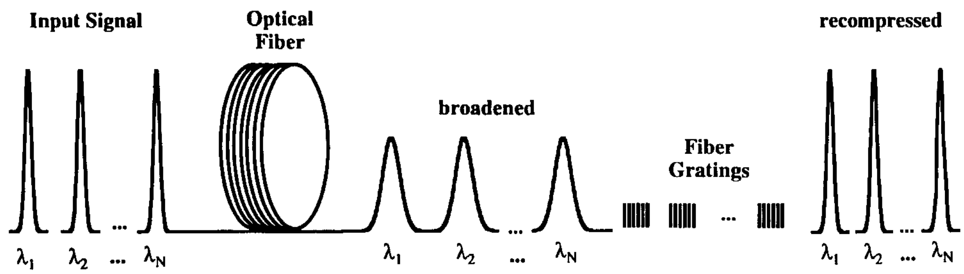

Fig. 3. Schematic illustration of a dispersion compensator designed for simultaneous compensation of GVD in WDM communication system by using multiple cascaded gratings.

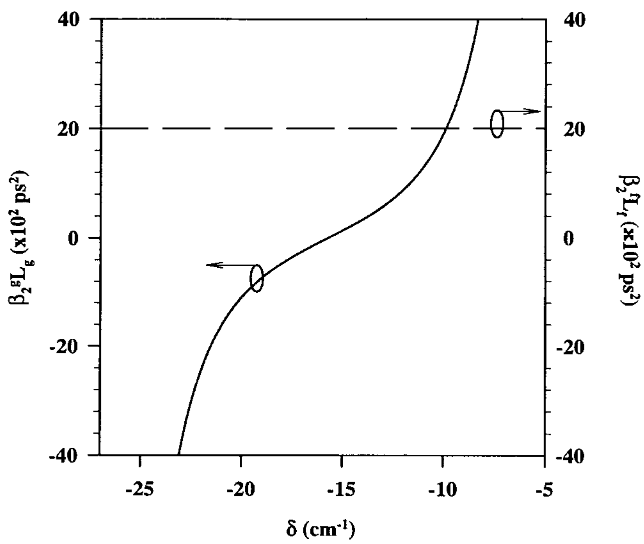

Fig. 4. Graphical solution of the design equation (6) for $L_f = 100$ km, $\beta_2^f = -20$ ps^2/km, $\kappa = 4$ cm^{-1}, $L_g = 40$ cm, and $\Delta\nu = 100$ GHz.

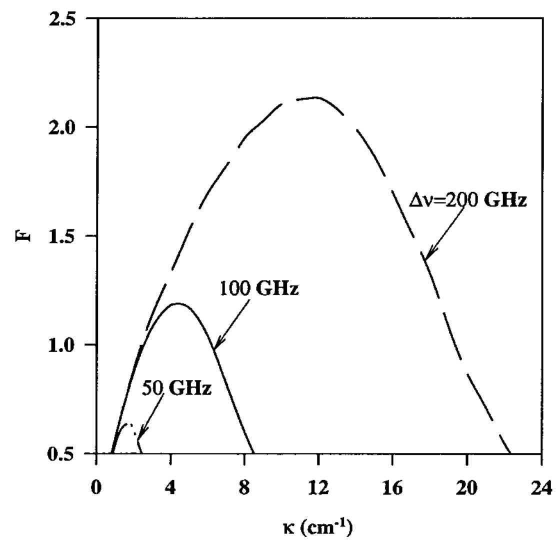

Fig. 6. Figure of merit F versus coupling coefficient with optimized detuning for each κ for $\Delta\nu = 200$ GHz (solid line), 100 GHz (dashed line), and 50 GHz (dot-dashed line).

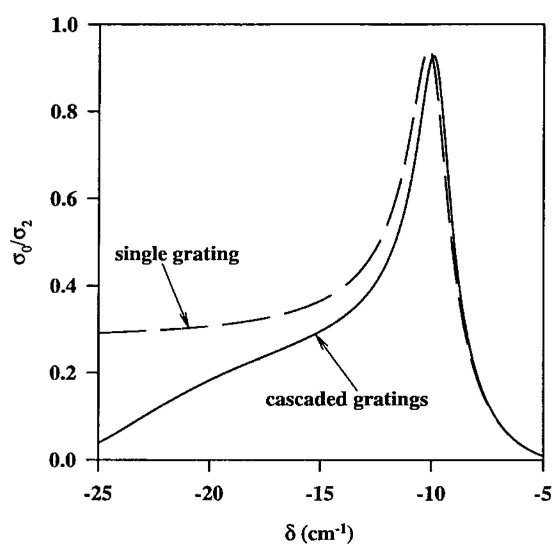

Fig. 5. Ratio σ_0/σ_2 for two cascaded gratings (solid line) and for the single grating case (dashed line).

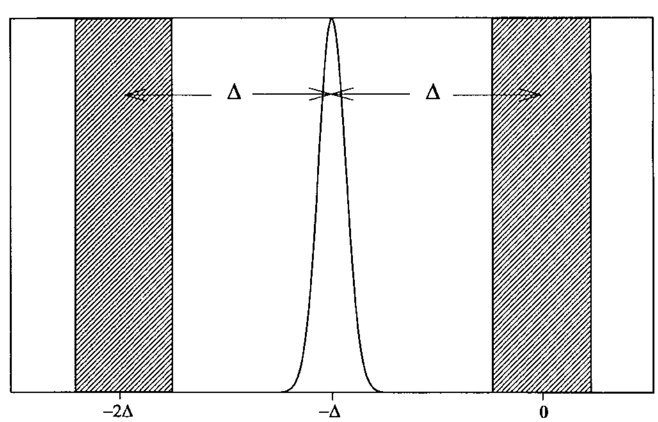

Fig. 7. Schematic illustration of the operation of an add–drop filter incorporating cascaded gratings. The channels located at 0 and -2Δ are added or dropped, but the channel located at $-\Delta$ is transmitted through both gratings.

by the third-order dispersion is given by [14]

$$\frac{\sigma}{\sigma_0} = \sqrt{1 + \frac{1}{8}\left(\frac{\beta_3^g L_g}{2\sigma_0^3}\right)^2}. \tag{8}$$

The broadening is negligible (less than 3%) if

$$\sigma_0 > \left(\frac{\beta_3^g L_g}{\sqrt{2}}\right)^{1/3}. \tag{9}$$

For given values of the channel spacing and coupling strengths (i.e., β_3^g is fixed and given by (4), where Δ should be doubled as shown in Fig. 7), minimum initial pulse width that can be used for undistorted transmission is proportional to the cubic

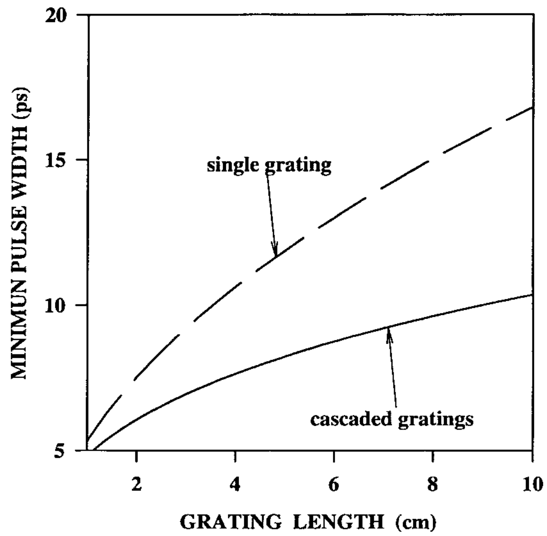

(a)

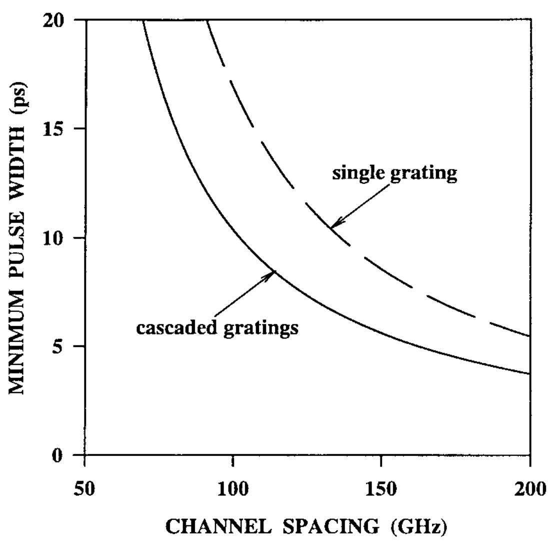

(b)

Fig. 8. (a) Minimum allowed initial pulse width as a function of grating length for two cascaded gratings (solid line) and a single grating (dashed line). (b) Minimum allowed initial pulse width as a function of the channel spacing plotted under the same conditions.

root of the grating length. Note that the optimal values of the coupling strength and the grating length are imposed by the system design. Fig. 8(a) shows minimum allowed initial pulse width defined by the equality in (9) $\sigma_{\min} = (\beta_3^g L_g/\sqrt{2})^{1/3}$ as a function of grating length and compares it to that defined in [8] for the single-grating case $\sigma_{\min} = \sqrt{2\beta_2^g L_g}$ for $\kappa = 11.8$ cm^{-1}, $\Delta = 31.4$ cm^{-1}. These results show that when gratings are cascaded the limitation on minimum pulse width (or maximum bit rate) is less strict for cascaded gratings. This is certainly a desirable feature of cascaded gratings and is due to the fact that $\beta_2^g = 0$ in the middle between two stop bands.

The minimum allowed pulse width is also limited by the channel spacing of WDM system. In Fig. 8(b), we plot minimum allowed initial pulse width as a function of channel spacing for given $\kappa = 11.8$ cm^{-1} and $L_g = 10$ cm. Again, we compare cascaded gratings (solid line) with a

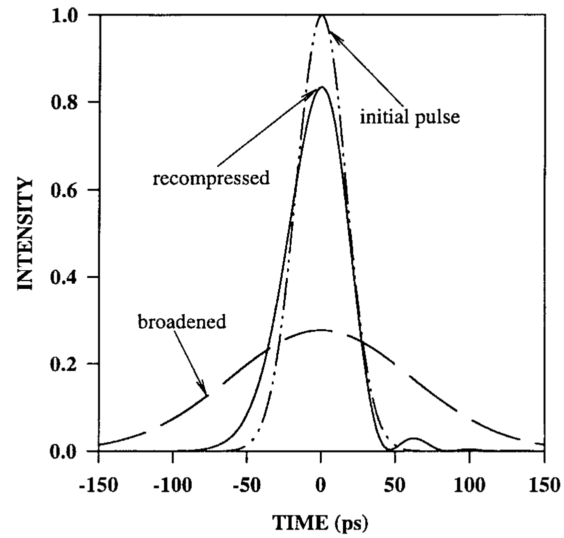

Fig. 9. Numerically simulated shapes of the initial, broadened, and recompressed pulses after transmission through 100 km of fiber and two 40-cm-long apodized gratings with $\kappa = 12$ cm^{-1}, $\Delta\nu = 200$ GHz.

single grating (dashed line). Fig. 8(b) shows that as channel spacing increases, the restriction on the initial pulse width becomes less severe. As an example, for a typical value of 75% for the bandwidth utilization parameter, defined as [4], [8]BWU $= \Delta_{3\,\mathrm{dB}}/\Delta$, where $\Delta_{3\,\mathrm{dB}} \approx 2\kappa$ is the channel 3 dB bandwidth and $\Delta = 31.4$ cm^{-1} the minimum allowed rms pulse width for cascaded gratings case is about 7.8 ps, while for the single grating case it is about 10.6 ps.

IV. Numerical Examples

A. Dispersion Compensation Using Cascaded Fiber Gratings

To check the validity of our analytical model under realistic practical conditions we have performed numerical simulation by using the coupled-mode equations and studied the effect of out-of-band grating dispersion on propagation of a Gaussian pulse. We consider a dispersion compensator for simultaneous compensation of GVD in a WDM system with a channel spacing $\Delta\nu = 200$ GHz (62.8 cm^{-1}) and a channel bit rate of 10 Gb/s. We assume propagation through a fiber length of 100 km. As we desire F to be as large as possible we choose $\kappa = 12$ cm^{-1} from Fig. 6. Using (6) we find the optimum detuning of the central frequency of the optical pulse from the grating at $\delta = 0$ to be $\delta_{\mathrm{opt}} = -22.2$ cm^{-1}. We assume that all gratings are apodized and have the same length ($L_g = 40$ cm) and the same coupling coefficient κ. We use apodization to remove the sidelobes in the grating reflection spectrum [3], [16]. It was shown previously that apodization does not change the amount of compression but improves the peak intensity of the recompressed pulse [3].

In Fig. 9, the input pulse, dispersion-broadened pulse at the fiber output, and recompressed pulse are shown. The recompressed pulse is slightly asymmetric and contains small oscillations on its trailing edge, the features that indicate the presence of some third-order dispersion at the optimal δ. There is a tradeoff between the quality of the output

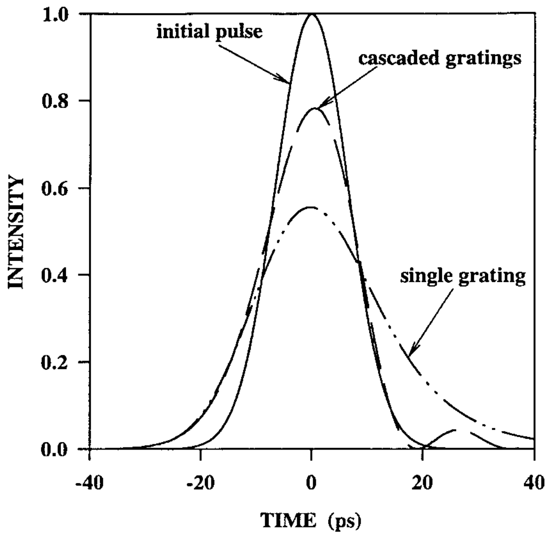

(a)

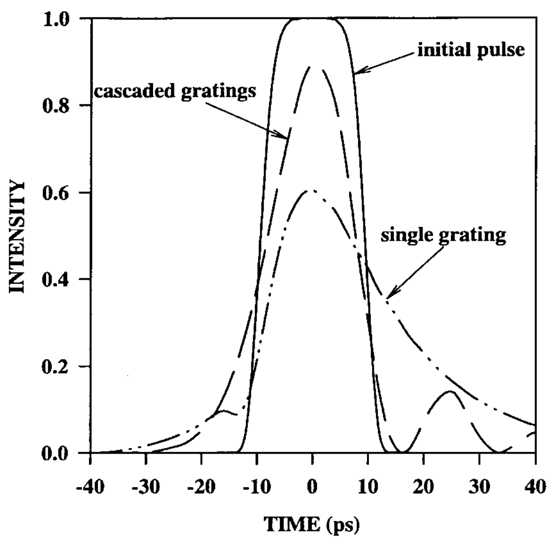

(b)

Fig. 10. Comparison of transmitted pulses when a Gaussian pulse (a) and a super-Gaussian pulse (b) propagated through the two cascaded gratings (dashed line) and a single grating (dot-dashed line). The input pulse is also shown by a solid line.

recompressed pulse, which improves for larger detunings δ, and the maximum compression ratio which decreases for larger δ because of the detrimental effect of the second grating.

B. Dispersion in Add/Drop Filters

In this example, we simulate numerically the transmission of a channel equally spaced ($\Delta = 31.4$ cm^{-1}) from the two adjacent apodized fiber gratings with $\kappa = 11.8$ cm^{-1} and $L_g = 10$ cm. In Fig. 10(a) we show the results of numerical simulations for propagation of 6.5 ps (rms-width) pulse in a system of two cascaded gratings (dashed line) and compare it with a single grating case (dot-dashed line). Note that in the latter case the transmitted pulse is affected by both GVD and third-order dispersion of a single fiber grating, while in a system of cascaded gratings the GVD is zero but the third-order dispersion is twice as much as that of a single grating. The broadened pulse is asymmetric with an oscillatory structure near its trailing edge, which is typical for pulse propagation in the medium with nonzero third-order dispersion at the zero-GVD wavelength [14]. From Fig. 8(a) we find that $\sigma_{\min} \approx 10.3$ ps for this case. Equation (8) shows that the initial pulse of width 6.5 ps will broaden by a factor of $\sqrt{2}$.

Finally, we simulated the transmission of 5.6 ps (rms-width) super-Gaussian pulse through the system of gratings described above. The initial (solid line) and broadened (dashed line) pulses are shown in Fig. 10(b). These results show that detrimental effect of the dispersion possessed by fiber grating is stronger for such square-like pulses.

V. Discussion and Conclusion

We have proposed a cascaded-grating-based dispersion compensator, operating in the transmission-mode, for dispersion compensation of multiple channels WDM lightwave systems. The performance of the compensator was analyzed using a simple analytical model based on the coupled-mode equations. The design of cascaded-grating-based dispersion compensator is complicated because the parameters should be chosen such that adjacent gratings do not significantly affect the performance of each other, implying a channel spacing $\Delta \gg 2\kappa$. As the four grating parameters κ, δ, L_g and Δ are coupled, they can not be chosen independently. It has been pointed out that grating GVD is high only in a limited range of detunings close to the edge of the stop band [3], of the order of the bandwidth of the grating. In our scheme, this limitation becomes even more severe, especially for dense WDM systems. As the channel spacing becomes smaller, the GVD changes more rapidly between the stop bands as shown in Fig. 1(a).

We also examined the dispersion properties of cascaded-grating-based add–drop filters. We extended the analysis of [8] and considered the effect of the dispersion on the adjacent channels transmitted through such add–drop filters. We have shown that for a channel transmitted at the zero-GVD wavelength, the performance is limited mostly by the third-order dispersion. However, the limitation on the minimum allowed pulse width (which determines the maximum allowed bit rate) is less strict when gratings are cascaded, compared with the single-grating case. Combining these results with those from [8] we conclude that the grating dispersion can affect the performance of a WDM network in two ways. First, in dense WDM systems with a single grating based add–drop filter the transmitted channel may be broadened due to GVD dispersion and the maximum allowed bit rate is inversely proportional to the quadratic root of the grating length [8]. Second, in WDM networks incorporating cascaded gratings, the transmitted channel may be distorted due to cubic dispersion and maximum achievable bit rate is inversely proportional to the cubic root of the grating length. We also showed numerically that the impact of the grating dispersion is even more severe for square-like (super-Gaussian) pulses, which are typically used in NRZ communication systems. These results suggest that the grating parameters should be carefully arranged to minimize the effect of out-of-band dispersion (both second and third order).

Finally, we note that our results may be also important in designing of recently proposed multiple-grating fiber structures for combined wavelength- and time-division multiplexing and the photonic code-division multiple-access networks [18], [19].

ACKNOWLEDGMENT

The authors would like to thank T. Erdogan, R. E. Slusher, T. A. Strasser, and G. Lenz for helpful comments. N. M. Litchinitser would like to acknowledge the Aileen S. Andrew Foundation for its postdoctoral support.

REFERENCES

[1] G. P. Agrawal, *Fiber-Optic Communication Systems*, 2nd ed. New York: Wiley, 1997.

[2] F. Ouellette, "Dispersion cancellation using linearly chirped Bragg grating filters in optical waveguides," *Opt. Lett.*, vol. 12, pp. 847–849, 1987.

[3] N. M. Litchinitser, B. J. Eggleton, and D. B. Patterson, "Fiber Bragg gratings for dispersion compensation in transmission: Theoretical model and design criteria for nearly ideal pulse recompression," *J. Lightwave Technol.*, vol. 15, pp. 1303–1313, 1997.

[4] T. A. Strasser, P. J. Chandonnet, J. DeMarco, C. E. Soccolich, J. R. Pedrazzani, D. J. DiGiovanni, M. J. Andrejco, and D. S. Shenk, "UV-induced fiber grating OADM devices for efficient bandwidth utilization," in *Proc. OFC'96*, postdeadline paper, PD8, 1996.

[5] H. Okayama, Y. Ozeki, and T. Kunii, "Dynamic wavelength selective add/drop node comprising tunable gratings," *Electron. Lett.*, vol. 33, pp. 881–882, 1997.

[6] P. St. J. Russell, "Bloch wave analysis of dispersion and pulse propagation in pure distributed feedback structures," *J. Mod. Opt.*, vol. 38, pp. 1599–1619, 1991.

[7] B. J. Eggleton, T. Stephens, P. A. Krug, G. Dhosi, Z. Brodzeli, and F. Ouellette, "Dispersion compensation over 100 km at 10 Gbit/s using a fiber grating in transmission," *Electron. Lett.*, vol. 32, pp. 1610–1611, 1996.

[8] B. J. Eggleton, G. Lenz, N. Litchinitser, D. B. Patterson, and R. E. Slusher, "Implications of fiber grating dispersion for WDM communication systems," *IEEE Photon. Technol. Lett.*, vol. 9, pp. 1403–1405, 1997.

[9] G. Nykolak, G. Lenz, B. J. Eggleton, and T. A. Strasser, "Impact of fiber grating on WDM system performance," in *Proc. OFC'98*, paper TuA3, 1998.

[10] J. E. Sipe, L. Poladian, and C. M. de Sterke, "Propagation through nonuniform Bragg gratings," *J. Opt. Soc. Amer. A*, vol. 11, pp. 1307–1320, 1994.

[11] H. Kogelnik and C. V. Shank, "Coupled-wave theory of distributed feedback lasers," *J. Appl. Phys.*, vol. 43, pp. 2327–2335, 1972.

[12] W. Chen and D. L. Mills, "Gap solitons and nonlinear optical response of superlattices," *Phys. Rev. Lett.*, vol. 58, pp. 160–163, 1987.

[13] B. J. Eggleton, R. E. Slusher, C. M. de Sterke, P. A. Krug, and J. E. Sipe, "Bragg grating solitons," *Phys. Rev. Lett.*, vol. 76, pp. 1627–1630, 1996.

[14] G. P. Agrawal, *Nonlinear Fiber Optics*. New York: Academic, 1995.

[15] D. Marcuse, "Pulse distortion in single-mode fibers, 3: Chirped pulses," *Appl. Opt.*, vol. 20, pp. 3573–3579, 1981.

[16] B. Malo, S. Theriault, D. C. Johnson, F. Bilodeau, J. Albert, and K. O. Hill, "Apodized in-fiber Bragg grating reflectors photoimprinted using a phase mask," *Electron. Lett.*, vol. 31, pp. 223–225, 1995.

[17] J. E. Sipe, B. J. Eggleton, and T. A. Strasser, "Dispersion characteristics of nonuniform Bragg gratings: Implications for WDM communication systems," *Opt. Commun.*, vol. 151, pp. 269–274, 1998.

[18] L. R. Chen, S. D. Benjamin, P. W. E. Smith, J. E. Sipe, and S. Juma, "Ultrashort pulse propagation in multiple-grating fiber structures," *Opt. Lett.*, vol. 22, pp. 402–404, 1997.

[19] H. Fathallah, S. LaRochelle, and L. A. Rusch, "Analysis of an optical frequency-hop encoder with strain-tuned Bragg gratings," in *Tech. Dig. "Bragg Gratings, Photosensitivity, and Poling in Glass Fibers and Waveguides: Applications and Fundamentals"*, BMG5, 1997.

Natalia M. Litchinitser received the M.S. degree in physics from Moscow State University, Russia, in 1993 and the Ph.D. degree from the Illinois Institute of Technology, Chicago, in 1997.

She joined The Institute of Optics at the University of Rochester, Rochester, NY, as a Postdoctoral Fellow in 1997. Her current areas of interest include nonlinear and fiber optics, fiber gratings, solitons, WDM systems, and dispersion compensation in optical communication systems.

Benjamin J. Eggleton received the Bachelor's degree with Honors in physics from the University of Sydney, Sydney, New South Wales, Australia. He received the Ph.D. degree from the School of Physics and the Optical Fiber Technology Center in the Australian Photonics Cooperative Research Center, at the University of Sydney in 1996. His doctoral research focused on linear and nonlinear effects in fiber gratings. The highlight of this research involved the first observation of nonlinear propagation effects in photonic bandgap structures

He joined the Department of Optical Physics at Bell Laboratories, Lucent Technologies, Murray Hill, NJ, in 1996. In July 1998, he joined the Optical Fiber Research Department at Bell Laboratories, as a Member of Technical Staff. His research interests include nonlinear optics, solitons, fiber optics, fiber gratings and photonic band-gap structures, all-optical switching devices and dispersion compensation techniques in WDM lightwaves systems.

Dr. Eggleton was awarded the 1997 Adolph Lomb Medal from the Optical Society of America for his research involving the first observation of nonlinear propagation effects in photonic bandgap structures.

Govind P. Agrawal (M'83–SM'86–F'96) received the B.S. degree from the University of Lucknow, India, in 1969 and the M.S. and Ph.D. degrees from the Indian Institute of Technology, New Delhi, in 1971 and 1974, respectively.

After holding positions at the Ecole Polytechnique, France, the City University of New York, NY, and AT&T Bell Laboratories, Murray Hill, NJ, he joined the Faculty of the Institute of Optics at the University of Rochester, Rochester, NY, in 1989, where he is a Professor of Optics. His research interests focus on quantum electronics, nonlinear optics, and laser physics. In particular, he has contributed significantly to the fields of semiconductor lasers, nonlinear fiber optics, and optical communications. He is an author or coauthor of more than 250 research papers, several book chapters and review articles, and three books *Semiconductor Lasers* (New York: Van Nostrand-Reinhold, 1993), *Nonlinear Fiber Optics* (New York: Academic, 1995), and *Fiber-Optic Communication Systems* (New York: Wiley, 1997). He has also edited the books *Contemporary Nonlinear Optics* (New York: Academic, 1992) and *Semiconductor Lasers: Past, Present and Future* (New York: AIP Press, 1995).

Dr. Agrawal is a Fellow of the Optical Society of America (OSA).